



Research article

Traumatic bone marrow edema of the calcaneus: Evaluation of color-coded virtual non-calcium dual-energy CT in a multi-reader diagnostic accuracy study



Christian Booz^a, Jochen Nöske^a, Moritz H. Albrecht^{a,*}, Lukas Lenga^a, Simon S. Martin^a, Julian L. Wichmann^a, Nicole A. Huizinga^c, Katrin Eichler^b, Nour-Eldin A. Nour-Eldin^b, Thomas J. Vogl^b, Ibrahim Yel^a

^a Division of Experimental Imaging, Department of Diagnostic and Interventional Radiology, University Hospital Frankfurt, Frankfurt am Main, Germany

^b Department of Diagnostic and Interventional Radiology, University Hospital Frankfurt, Frankfurt am Main, Germany

^c Interdisciplinary Center for Neuroscience, Goethe-University of Frankfurt, Frankfurt am Main, Germany

ARTICLE INFO

Keywords:

Multidetector computed tomography

Magnetic resonance imaging

Calcaneus

Fractures

Bone

Dual-Energy CT

ABSTRACT

Purpose: To investigate the diagnostic accuracy of dual-energy computed tomography (CT) virtual non-calcium (VNCa) reconstructions for the depiction of traumatic bone marrow edema of the calcaneus.

Method: Data from 62 patients (33 women, 29 men; mean age: 41 years, range: 19–84 years) with acute tarsal trauma who had undergone third-generation dual-source dual-energy CT and 3-T magnetic resonance imaging (MRI) within seven days between January 2017 and July 2018 were retrospectively analyzed. Five radiologists, blinded to clinical and MRI information, independently assessed conventional grayscale dual-energy CT series for the presence of fractures; after at least eight weeks, readers re-evaluated all cases using color-coded VNCa reconstructions for the presence of bone marrow edema. Quantitative analysis of CT numbers on VNCa reconstructions was performed by a sixth radiologist. Two additional experienced radiologists, blinded to clinical and CT information, assessed MRI series in consensus to define the reference standard. Sensitivity, specificity and the area under the curve (AUC) were the primary indices for diagnostic accuracy.

Results: MRI revealed 62 areas with bone marrow edema in 39 patients. In the qualitative analysis, VNCa showed high overall sensitivity (286/310 [92%]) and specificity (899/930 [97%]) for the depiction of bone marrow edema. A cut-off value of –53 Hounsfield units (HU) provided a sensitivity of 82% (51/62) and specificity of 95% (176/186) for differentiating bone marrow edema. The overall AUC was 0.98.

Conclusions: In both quantitative and qualitative analyses, dual-energy CT VNCa reconstructions show excellent diagnostic accuracy for the visualization of traumatic calcaneal bone marrow edema compared to MRI.

1. Introduction

Bone marrow edema is frequently associated with disability, instability and soft tissue lesions such as tendinous and ligamentous injuries; therefore it entails substantial social and economic burden [1–3]. Complications of traumatic bone marrow edema such as dislocation, chondrolysis and osteoarthritis can result in irreversible morbidity and long recovery time [1,4,5]. Thus, accurate and early diagnosis is required for optimal therapy to prevent poor patient outcome [1].

Magnetic resonance imaging (MRI) is the diagnostic imaging method of choice for the depiction of traumatic bone marrow edema [6]. However, there are limitations of MRI in clinical routine. There are absolute and relative contraindications, including cochlear implants, pacemakers, claustrophobia and the inability to lie still during image acquisition. The availability of MRI is frequently limited outside of regular working hours. In addition, MRI is expensive and time-consuming compared to computed tomography (CT). Therefore, it is common for patients with acute tarsal trauma to initially undergo CT in

Abbreviations: AUC, area under the curve; CT, computed tomography; HU, Hounsfield unit; MRI, magnetic resonance imaging; MSK, musculoskeletal; NPV, negative predictive value; PD, proton density; PPV, positive predictive value; ROC, receiver-operating characteristic; ROI, region of interest; VNCa, virtual non-calcium

* Corresponding author at: University Hospital Frankfurt, Division of Experimental Imaging, Department of Diagnostic and Interventional Radiology, Theodor-Stern-Kai 7, 60590 Frankfurt am Main, Germany.

E-mail address: experimentalimaging@gmail.com (M.H. Albrecht).

<https://doi.org/10.1016/j.ejrad.2019.07.023>

Received 6 March 2019; Received in revised form 22 June 2019; Accepted 18 July 2019

0720-048X/© 2019 Elsevier B.V. All rights reserved.

cases with suspected fracture despite a negative x-ray [7].

While conventional grayscale CT allows for detection of fractures, the visualization of traumatic bone marrow edema is impeded by the overlying trabecular bone [4,5]. Although osseous structures can be removed virtually on single-energy CT images by dedicated algorithms, these postprocessing algorithms do not permit depiction of bone marrow as a result of the non-resolvable surrounding trabecular structures [8]. In this context, dual-energy CT enables material discrimination by exploiting the energy dependence of the photoelectric effect at different x-ray spectra [9–15]. Thereby, dual-energy CT allows for three-material decomposition and calculation of color-coded virtual non-calcium (VNCa) images [9,10]. Previously, VNCa reconstructions have been shown to provide direct visualization of bone marrow edema with high diagnostic accuracy and to depict bone marrow infiltration in patients with multiple myeloma [16–20]. Guggenberger showed promising results using VNCa reconstructions derived from first-generation dual-source dual-energy CT for the detection of traumatic bone marrow edema of the ankle [21]. With the advent of third-generation dual-source dual-energy CT, an optimized VNCa reconstruction algorithm established for the depiction of bone marrow edema has been created and integrated into the postprocessing software. However, no studies to date have investigated the diagnostic accuracy of this reconstruction algorithm for the depiction of traumatic bone marrow edema of the calcaneus.

We hypothesized that color-coded VNCa images reconstructed from third-generation dual-source dual-energy CT may yield high diagnostic accuracy and confidence for detecting bone marrow edema in patients with acute tarsal trauma. The purpose of our multireader study was to investigate the diagnostic accuracy of a novel color-coded dual-energy CT VNCa reconstruction algorithm for the depiction of traumatic bone marrow edema of the calcaneus with MRI serving as the reference standard.

2. Material and methods

This retrospective study was approved by the institutional review board. The requirement to obtain written informed consent was waived. The institutional review board approved the chart review.

2.1. Patient selection and study design

A total of 86 consecutive patients with acute tarsal trauma who had undergone clinically indicated non-contrast dual-energy CT and MRI examinations between January 2017 and July 2018 were initially considered for study inclusion. Only patients with an examination interval of up to 7 days ($n = 73$) were included to ensure comparability. No more specific inclusion criteria were applied. Exclusion criteria were malignancy of the tarsus ($n = 2$), infection of the tarsus ($n = 1$), patients with metal implants in the tarsus ($n = 6$), and previous local surgery within 1 year ($n = 2$). Thus, 62 patients were ultimately evaluated (Fig. 1). Indications for the examinations in this study were distortion ($n = 23$), fall ($n = 21$), and motor vehicle accident ($n = 18$).

2.2. Dual-energy CT protocol

CT scans were performed on a third-generation dual-source dual-energy CT system (Somatom Force; Siemens Healthineers, Forchheim, Germany). Both x-ray tubes were operated at different kilovoltage settings (tube A: 90 kVp, 180 mAs; tube B: Sn150 kVp [0.64 mm tin filter], 180 mAs). Each scan was performed in craniocaudal direction without administration of intravenous contrast agent and by application of a dual-energy protocol (rotation time, 500 msec; pitch, 0.6; collimation, 192 x 0.6 mm). Automatic attenuation-based tube current modulation (CARE dose 4D; Siemens Healthineers) was used. Mean volume CT dose index was $10.4 \text{ mGy} \pm 3.2$ (range, 3.9–13.5 mGy), and mean dose-length product was $179.4 \text{ mGy} \cdot \text{cm} \pm 55.5$ (range,

86.6–357.1 mGy · cm).

2.3. CT image reconstruction and postprocessing

Three different image sets were acquired in each CT examination: 90 kVp, Sn150 kVp, and weighted average (ratio, 0.5:0.5) to resemble the contrast properties of a single-energy 120 kVp image [22]. For conventional fracture detection, image series (axial, coronal and sagittal: section thickness 1 mm, increment 0.75 mm) were reconstructed with a dual-energy bone kernel (Br69f). For color-coded visualization of bone marrow edema, reconstructions (axial, coronal and sagittal: section thickness 1 mm, increment 0.75 mm) were created with a dual-energy medium-soft convolution kernel (Qr40, advanced model-based iterative reconstruction [ADMIRE] level of 3) for the high- and low-kilovolt series. Color-coded VNCa images were reconstructed on a commercially available three-dimensional workstation (syngo.via version VB30A; Siemens Healthineers) by application of three-material decomposition differentiating calcium, fat and water. The VNCa reconstructions were displayed using standard dual-energy bone marrow settings (Fig. 2). For the image analysis, axial, sagittal and coronal VNCa reconstructions and conventional grayscale CT series were sent to the picture archiving and communication system (PACS).

2.4. MRI protocol

MRI scans were performed on a 3-T system (Magnetom PrismaFit; Siemens Healthineers) with a dedicated foot coil. Standard coronal proton density (PD)-weighted turbo spin-echo with fat saturation (repetition time msec/echo time msec, 2830/33; matrix size, 384×307 ; section thickness, 3 mm), sagittal PD-weighted turbo spin-echo with fat saturation (repetition time msec/echo time msec, 2800/38; matrix size, 384×307 ; section thickness, 3 mm), axial PD-weighted turbo spin-echo with fat saturation (repetition time msec/echo time msec, 2850/27; matrix size, 384×290 ; section thickness, 3 mm) and coronal T1-weighted turbo spin-echo (repetition time msec/echo time msec, 736/12; matrix size, 384×307 ; section thickness, 3 mm) sequences were performed.

2.5. Multireader image analysis

All image analyses were performed on a conventional PACS workstation (Centricity 4.2; GE Healthcare). For qualitative and quantitative image analysis, the calcaneus was divided into four regions (lateral, central, medial and sustentacular) according to the Sanders classification system of calcaneal fractures [23].

In order to establish the reference standard, two radiologists (X.X.X. and X.X.X. [head of department and managing consultant] with 32 and 20 years of experience in musculoskeletal [MSK] imaging) assessed MRI series in consensus for the presence of traumatic bone marrow edema by applying a binary classification (0 = normal bone marrow; 1 = bone marrow edema). The readers were blinded to clinical or dual-energy CT information and were allowed to adjust window settings. The entire amount of MRI sequences could be evaluated. Furthermore, image quality, image noise and diagnostic confidence were rated individually by using five-point Likert scales (range 1–5; 1 = unacceptable, 5 = excellent).

Subsequently, five radiologists (X.X.X., board-certified radiologist with 8 years of experience in MSK imaging; X.X.X., radiology resident with 5 years of experience in MSK imaging; X.X.X., radiology resident with 5 years of experience in MSK imaging; X.X.X., radiology resident with 3 years of experience in MSK imaging; X.X.X., radiology resident with 3 years of experience in MSK imaging), independently analyzed axial, coronal and sagittal dual-energy CT series. Readers were blinded to clinical or MRI information. First, conventional grayscale CT series were presented in random order (bone window settings; width, 2700 Hounsfield units (HU); level, 700 HU). Radiologists assessed the

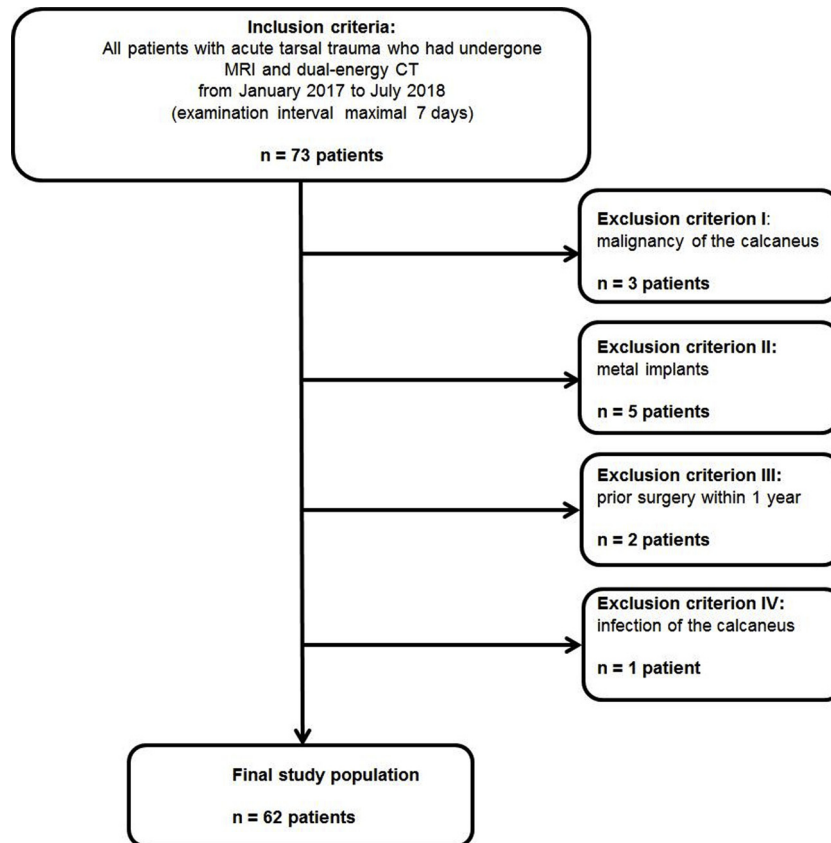


Fig. 1. Flowchart of study enrollment based on Standards for Reporting of Diagnostic Accuracy Studies (STARD).

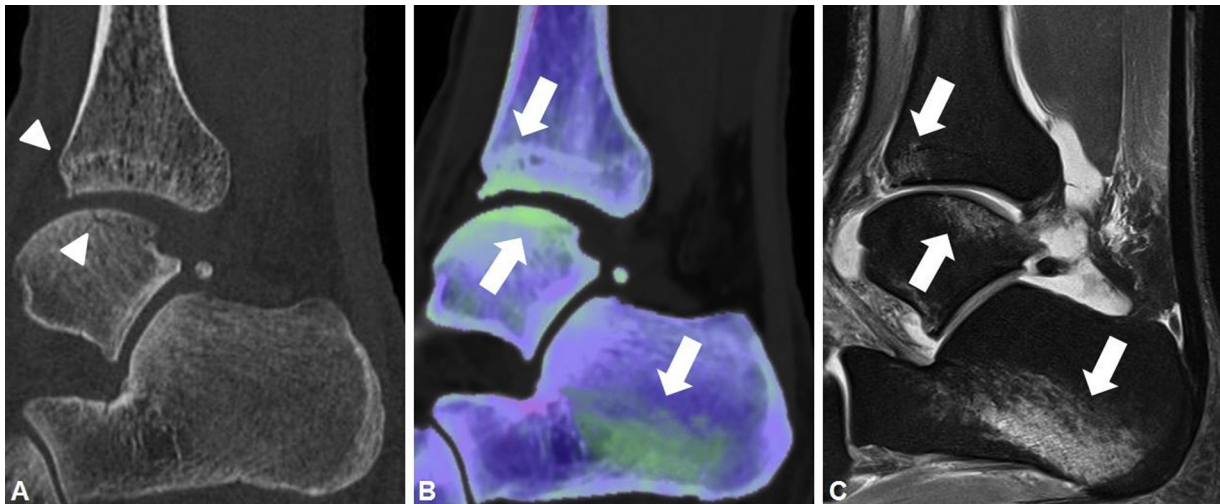


Fig. 2. Dual-energy computed tomography (CT) and magnetic resonance imaging (MRI) performed in a 37-year-old man presenting with right-sided acute tarsal trauma after motor vehicle accident. (A) In sagittal conventional grayscale CT series, fractures of the tibia and talus (*arrowheads*) were detected by all five CT readers in this study. Osseous structures of the calcaneus were assessed as intact by all readers. (B) Reconstruction of sagittal color-coded virtual non-calcium (VNCA) series using a three-material decomposition algorithm that differentiates calcium, fat and water, was performed on a commercially available three-dimensional workstation and the VNCA reconstruction displayed using standard dual-energy bone marrow settings. The sagittal color-coded VNCA series showed distinct traumatic bone marrow edema (displayed as green area, *arrows*) of tibia, talus and calcaneus (detected by 5/5 readers). (C) Additionally performed sagittal proton density (PD)-weighted magnetic resonance imaging (MRI) series confirmed the diagnosis of traumatic bone marrow edema of the calcaneus.

presence and type of fractures according to the Sanders classification system of calcaneal fractures [19]. Following a reading interval of eight weeks to avoid recall bias, all radiologists evaluated randomly-ordered, color-coded VNCA reconstructions for the presence of traumatic bone marrow edema on a per-region basis and on a per-patient basis. Evaluations were made without access to conventional grayscale CT data

and used the previously described binary classification. Thereby, the radiologists were permitted to adjust window settings and scroll through the entire stack of CT series. Considering artifacts from beam hardening, filtering effects and removal of the cortex, only traumatic bone marrow edema greater than 3 mm in distance from the cortical bone were included [24]. Diagnostic confidence, image quality and

image noise in all CT series were assessed using the aforementioned five-point Likert scales.

During quantitative image analysis, CT numbers were measured on axial color-coded VNCA images by placing circular regions of interest (ROI, 8 mm diameter) in each region according to the Sanders classification system of calcaneal fractures by a sixth blinded reader (X.X.X., senior year medical student with two years of experience in MSK imaging) [23]. In each region, the ROI was placed at the highest signal intensity on VNCA reconstructions. In regions without evidence of bone marrow edema, the ROI was positioned in the center of the region.

2.6. Statistical analysis

All statistical analyses were performed using dedicated software (SPSS Statistics for Windows, version 23.0, IBM, Armonk, NY; MedCalc for Windows, Version 13, MedCalc, Mariakerke, Belgium). The normality of data was assessed using the Kolmogorov-Smirnov test. Variables were expressed as means \pm standard deviations and assessed with the Wilcoxon matched-pairs test.

In the qualitative image analysis, sensitivity, specificity, positive predictive and negative predictive values (PPV and NPV) and accuracy values of color-coded VNCA reconstructions for the depiction of traumatic bone marrow edema of the calcaneus were computed on a per-region and per-patient basis. Clustering of regions per patient following the proposed method by Genders for each reader and for consensus analysis was taken into account [25]. Logistic regression analysis with a robust variance estimator was applied. Inter-reader agreement was evaluated by computing weighted Fleiss' κ according to Landis and Koch [26]. Receiver-operating characteristic (ROC) curve analysis and the area under the curve (AUC) were used to evaluate quantitative CT numbers derived from VNCA reconstructions on a per-region basis to define the optimal cut-off CT numbers for differentiation of traumatic bone marrow edema of the calcaneus. Based on these cut-off values, sensitivity and specificity values were calculated. Values of overall sensitivity, specificity, PPV, NPV and accuracy were expressed as means. The statistically significant difference was indicated by a p value less than 0.05. Mean ages were given as patient-level means.

3. Results

A total of 248 regions in 62 patients (mean age, 41 \pm 12 years; range, 19–84 years; mean BMI, 22 \pm 5 kg/m²; range 17–34 kg/m²) were assessed (Table 1), consisting of 33 women (53%; mean age, 43 \pm 11 years; range, 23–84 years; mean BMI, 22 \pm 3 kg/m²; range, 18–34 kg/m²) and 29 men (47%; mean age, 39 \pm 10 years; range, 19–78 years; mean BMI, 23 \pm 5 kg/m²; range, 17–29 kg/m²). Conventional grayscale CT revealed 13 calcaneal fractures in 11 patients according to the Sanders classification system of calcaneal fractures (median per patient, 0; range, 0–2) [19]. MRI revealed 62 regions with traumatic bone marrow edema (16 lateral, 15 central, 14 medial, 17 sustentacular edema) in 39 patients (median per patient, 1; range, 0–2).

Table 1

Characterization of the patient population in this study.

Characteristics	Value
Number of patients	62
Mean age \pm SD, range	41 \pm 11, 19–84
Mean BMI \pm SD, range	22 \pm 5, 17–34
Women	33/62 (0.53)
Mean age of women \pm SD, range	43 \pm 11, 23–84
Mean BMI of women \pm SD, range	22 \pm 3, 18–34
Men	29/62 (0.47)
Mean age of men \pm SD, range	39 \pm 10, 19–78
Mean BMI of men \pm SD, range	23 \pm 5, 17–29
Number of patients with known osteoporosis	4/62 (0.06)

Mean examination interval between CT and MRI was three days (range, 0–6 days). All exams showed diagnostic image quality.

3.1. Diagnostic accuracy per region

The region-based qualitative image analysis revealed an excellent overall sensitivity (286/310 [92%]), specificity (899/930 [97%]), PPV (286/317 [90%]), NPV (899/923 [97%]) and accuracy (1185/1240 [96%]) of color-coded VNCA reconstructions for the depiction of traumatic calcaneal bone marrow edema. Overall inter-reader agreement was excellent for VNCA images ($\kappa = 0.84$). Overall sensitivity was significantly lower regarding medial calcaneal regions (63/70 [90%]) compared to lateral (75/80 [94%]), central (74/80 [93%]) and sustentacular calcaneal regions (79/85 [93%]) ($p < .001$, respectively). Overall specificity was significantly decreased for lateral (221/230 [96%]) and central calcaneal regions (222/230 [97%]) compared to medial (236/240 [98%]) and sustentacular calcaneal regions (220/225 [98%]) ($p < .001$, respectively). Notably, the most experienced CT reader in this study (board-certified radiologist with 8 years of experience in MSK imaging) was able to achieve similar overall diagnostic performance in the detection of traumatic bone marrow edema as with MRI (sensitivity, specificity, PPV, NPV and accuracy, all $\geq 95\%$) (Table 2). An example case demonstrating direct visualization of traumatic bone marrow edema of the calcaneus by using color-coded VNCA reconstructions is shown in Fig. 3.

Quantitative image analysis showed a significant difference between CT numbers on VNCA reconstructions in regions with and without traumatic bone marrow edema of the calcaneus ($p < .001$) (Fig. 4). The ROC curve analysis revealed an optimal cut-off value of -53 HU with a sensitivity of 82% (51/62 positive regions) and specificity of 95% (176/186 negative regions) for differentiating traumatic bone marrow edema of the calcaneus. The overall AUC was 0.98 (Fig. 5) and the overall Youden's J index was 0.86. Results of the quantitative image analysis of CT numbers in each region are shown in Table 3.

3.2. Diagnostic accuracy per patient

The patient-based qualitative image analysis demonstrated high overall sensitivity (185/195 [95%]), specificity (106/115 [92%]), PPV (185/194 [95%]), NPV (106/116 [91%]) and accuracy (291/310 [94%]) of color-coded VNCA reconstructions for the depiction of traumatic bone marrow edema of the calcaneus in comparison to MRI. The overall inter-reader agreement was excellent for VNCA images ($\kappa = 0.87$). Patient-based diagnostic accuracy results of each CT reader using color-coded VNCA reconstructions for the depiction of traumatic bone marrow edema of the calcaneus are summarized in Table 4.

3.3. Image rating

All readers in this study reported high diagnostic confidence for both the assessment of traumatic bone marrow edema of the calcaneus in MRI series (mean score: 4.39) and VNCA reconstructions (mean score: 4.34) without significant difference ($p = 0.09$) (Fig. 6). In this context, the inter-reader agreement was excellent for VNCA reconstructions ($\kappa = 0.86$) and MRI series ($\kappa = 0.89$).

There was no significant difference ($p = 0.34$) between reader ratings for the image noise in MRI series (mean score: 4.18) and in VNCA reconstructions (mean score: 4.16). Inter-reader agreement was excellent for VNCA ($\kappa = 0.85$) and MRI ($\kappa = 0.87$).

The image quality was assessed with mean scores of 4.52 (MRI series) and 4.40 (VNCA reconstructions), revealing a significant difference between both imaging modalities (comparison, $p < .001$). Again, inter-reader agreement was excellent for VNCA ($\kappa = 0.84$), and MRI ($\kappa = 0.88$).

Table 2

Region-based diagnostic accuracy results of each CT reader using color-coded VNcA reconstructions for the detection of traumatic calcaneal bone marrow edema.

	Sensitivity	Specificity	PPV	NPV	Accuracy
Average	286/310 (0.92) [0.88-0.96]	899/930 (0.97) [0.94-0.99]	286/317 (0.90) [0.86-0.94]	899/923 (0.97) [0.95-1.00]	1185/1240 (0.96) [0.92-0.99]
Reader 1	59/62 (0.95) [0.90-0.99]	184/186 (0.99) [0.96-1.00]	59/61 (0.97) [0.92-0.99]	184/187 (0.98) [0.94-1.00]	243/248 (0.98) [0.94-1.00]
Reader 2	58/62 (0.94) [0.86-0.98]	180/186 (0.97) [0.91-0.99]	58/64 (0.91) [0.83-0.96]	180/184 (0.98) [0.91-1.00]	238/248 (0.96) [0.92-0.99]
Reader 3	59/62 (0.95) [0.90-0.99]	178/186 (0.96) [0.91-0.99]	59/67 (0.88) [0.81-0.93]	178/181 (0.98) [0.92-1.00]	237/248 (0.96) [0.92-0.99]
Reader 4	56/62 (0.90) [0.80-0.98]	178/186 (0.96) [0.90-0.99]	56/64 (0.88) [0.82-0.94]	178/184 (0.97) [0.94-1.00]	234/248 (0.94) [0.90-0.99]
Reader 5	54/62 (0.87) [0.82-0.92]	179/186 (0.96) [0.93-1.00]	54/61 (0.89) [0.83-0.94]	179/187 (0.96) [0.92-1.00]	233/248 (0.94) [0.90-0.98]

PPV: positive predictive value, NPV: negative predictive value. Statistical measures are given as fractions and as decimal values (round brackets). Numbers in square brackets are confidence intervals.

Notably, the most experienced CT reader in this study (reader 1) was able to achieve similar diagnostic performance in the detection of traumatic calcaneal bone marrow edema using VNcA reconstructions as with MRI (sensitivity, specificity, PPV, NPV and accuracy, all $\geq 95\%$). Reader 1 (board-certified radiologist) had 8 years of experience in musculoskeletal (MSK) imaging; reader 2 (radiology resident), 5 years; reader 3 (radiology resident), 5 years; reader 4 (radiology resident), 3 years; reader 5 (radiology resident), 3 years.

4. Discussion

The results of our study demonstrate the clinical applicability and high diagnostic accuracy of color-coded dual-energy CT VNcA reconstructions for the visualization of traumatic bone marrow edema of the calcaneus compared to MRI. In particular, the most experienced CT reader in this study was able to achieve excellent diagnostic accuracy (sensitivity, specificity, PPV, NPV and accuracy, all $\geq 95\%$). Furthermore, the excellent inter-reader agreement indicates high reliability of this reconstruction algorithm. Color-coded VNcA reconstructions achieved comparable ratings for diagnostic confidence and image noise to MRI without significant differences. In addition, the quantitative image analysis yielded a high correlation between CT numbers and MRI indicative of traumatic calcaneal bone marrow edema.

Previous studies have demonstrated high diagnostic accuracy of color-coded dual-energy CT-derived VNcA images for depicting bone marrow edema [15–17]. Guggenberger et al showed promising results for the visualization of traumatic bone marrow edema of the ankle by usage of VNcA reconstructions derived from second-generation dual-source dual-energy CT. The authors experimentally modified a post-processing algorithm which had been initially developed for liver

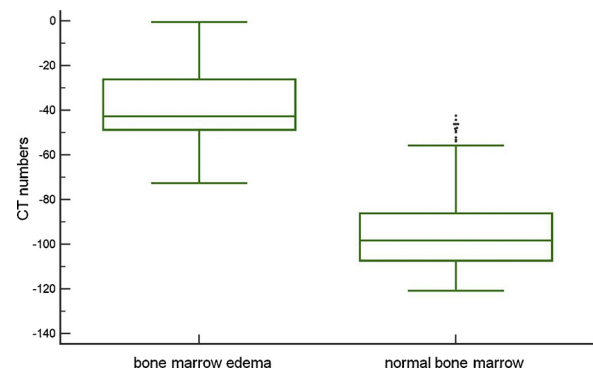


Fig. 4. Box plot of region-based mean CT numbers of calcaneal regions with and without bone marrow edema. The quantitative image analysis revealed a significant difference of CT numbers in regions with or without bone marrow edema ($p < .001$).

analysis [21]. Moreover, dedicated VNcA postprocessing reconstruction algorithms for the analysis of bone marrow edema have been established and integrated into software related to third-generation dual-

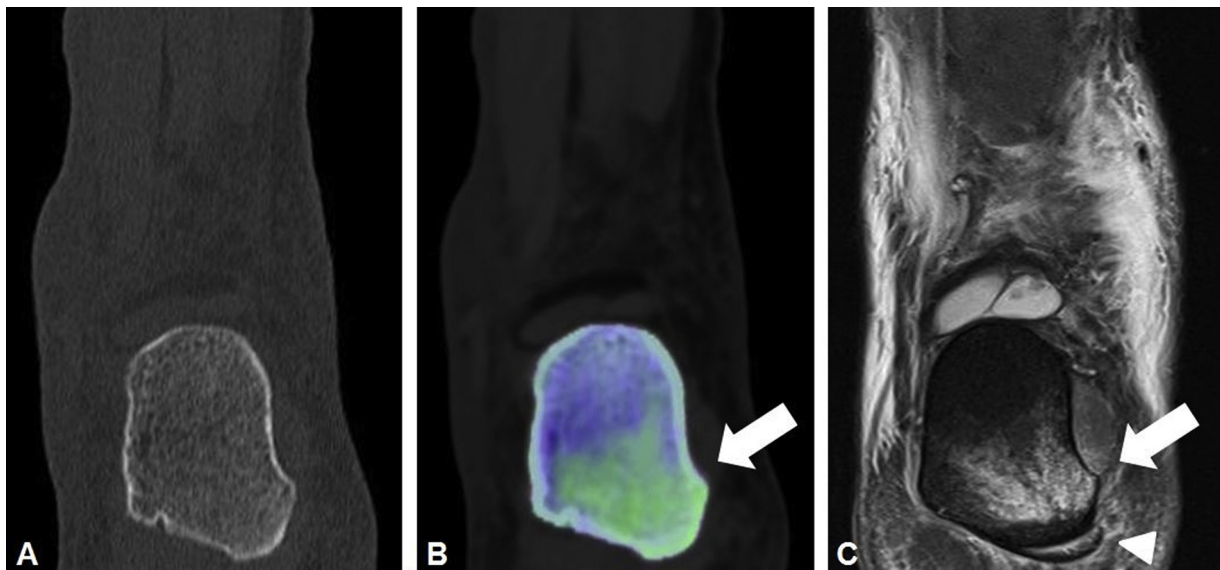


Fig. 3. Dual-energy computed tomography (CT) and magnetic resonance imaging (MRI) performed in a 35-year-old man presenting with right-sided acute tarsal trauma after fall. (A) In coronal conventional grayscale computed tomography (CT) series no fracture was detected. Osseous structures were assessed as intact by all five CT readers. (B) Additional reconstructed coronal color-coded virtual non-calcium (VNcA) series showed distinct traumatic bone marrow edema (displayed in green, arrow) of the calcaneus involving the medial cortical bone (detected by 5/5 CT readers). (C) MRI was performed due to the location of bone marrow edema with suspicion of associated ligamentous injuries and corresponding clinical signs. Coronal PD-weighted series confirmed the diagnosis of traumatic bone marrow edema and revealed grade 2 lesion of the plantar aponeurosis (arrowhead).

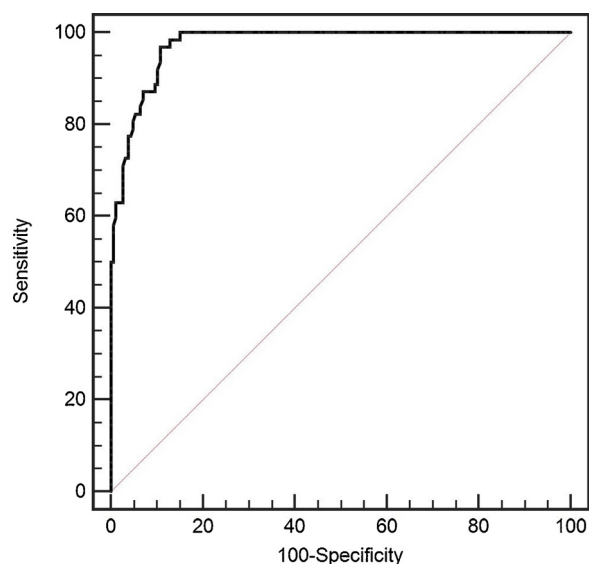


Fig. 5. Representative receiver operating characteristic curve calculated from overall CT numbers in the calcaneus (AUC = 0.98).

source dual-energy CT. In addition, technical advancements in scanner technology facilitate greater spectral separation with voltage settings of both x-ray tubes up to 90 kV and Sn150 kV for a more precise tissue and material decomposition compared to previous hardware [27]. Furthermore, an increased tube current flux up to 1500 mAs per tube lessens noise compared to former dual-source CT generations [16]. To date, no previous studies have examined dedicated color-coded VNCA reconstructions derived from third-generation dual-source dual-energy CT in patients with acute tarsal trauma.

The results of this study show higher diagnostic accuracy of VNCA reconstructions for the assessment of traumatic bone marrow edema compared to studies that investigated VNCA reconstructions acquired with first- and second-generation dual-source dual-energy CT scanners for analyzing bone marrow edema of the knee and ankle region [21,24]. This improvement may be explained partly by the described technical advancements of third-generation dual-source dual-energy CT scanner compared to former dual-source CT scanner generations. Interestingly, the calculated optimal cut-off CT number of -53 HU for the differentiation of calcaneal bone marrow edema is in accordance with cut-off CT numbers in previous studies investigating the knee and ankle region [21,24]. Notably, the sensitivity was significantly lowered in the medial region compared to the central, lateral and sustentacular regions in this study.

Patients with acute trauma of the ankle joint and the tarsus commonly undergo both CT and MRI in case of suspected undisplaced fractures and associated ligamentous injuries, because subtle fractures are frequently only detectable through the visualization of bone

marrow edema. Our study demonstrated high diagnostic accuracy of color-coded VNCA reconstructions for visualization of traumatic calcaneal bone marrow edema indicates that third-generation dual-source dual-energy CT may serve as a viable alternative imaging modality for patients with contraindications to MRI or in circumstances where MRI is not or restrictedly available (for instance, outside regular radiology department hours). Even in conditions where MRI would be available, our investigated CT approach may also have the potential to serve as a fast, accurate and widely available alternative for patients with acute tarsal trauma and suspected bone marrow edema. The need for an additional MRI exam, including repeated patient transport and positioning, may be obviated which could result in a more time-efficient workflow, reduced costs and improved patient comfort. Furthermore, in cases where an MRI examination would not be sufficiently indicated, the excellent diagnostic accuracy of VNCA reconstructions suggests that additional clinical relevant information (in comparison to conventional grayscale CT) can be routinely obtained in patients with tarsal trauma undergoing CT, since location and shape of bone marrow edema allow for the prediction of associated soft tissue injuries such as ligamentous tears [5]. Notably, the reconstruction of color-coded VNCA images derived from dual-energy CT lasted two minutes on average, further supporting its applicability in clinical routine.

There are limitations of our study that need to be addressed. First, we chose a close examination interval to prevent statistical distortion and therefore, only 62 patients were included. Second, CT readers independently analyzed conventional grayscale CT series initially in all patients. The evaluation of color-coded VNCA reconstructions regarding traumatic bone marrow edema was performed after a time interval of 8 weeks in each case. This sequence was not randomized, possibly causing statistical distortion. Third, bone marrow alterations can be caused by several reasons, such as primary bone tumor, bone metastasis, bone infarction, trauma or osteoarthritis [4,28]. To the best of our knowledge, none of these findings were present in our study. However, pathological causes of bone marrow edema, apart from trauma, cannot be entirely eliminated. Due to the temporal relationship with acute trauma in all patients in this study, bone marrow changes were most likely caused by traumatic microfractures and consecutive bone marrow edema. Fourth, the investigated VNCA reconstruction algorithm is currently only compatible with the vendor-specific dual-source CT technique and postprocessing software. Therefore, results and conclusions of this study are not yet applicable to dual-energy CT systems from other manufacturers.

5. Conclusions

Our study demonstrated that color-coded third-generation dual-source dual-energy CT VNCA reconstructions yield excellent diagnostic accuracy, as well as both equivalent diagnostic confidence and image noise compared to MRI for the assessment of traumatic calcaneal bone marrow edema in patients with acute tarsal trauma. Therefore, this

Table 3

Results of the quantitative image analysis of VNCA reconstructions for lateral, central, medial, medial and sustentacular calcaneal regions.

	Lateral	Central	Medial	Sustentacular	Overall
Mean CT number					
Positive regions	-35.7 ± 14.5	-41.1 ± 12.2	-40.2 ± 16.1	-40.6 ± 20.5	-39.2 ± 16.0
Negative regions	-93.2 ± 19.9	-93.2 ± 19.9	-93.2 ± 16.5	-94.2 ± 18.5	-92.9 ± 18.7
AUC	0.98 [0.96-1.00]	0.98 [0.95-1.00]	0.99 [0.95-1.00]	0.97 [0.93-1.00]	0.98 [0.95-1.00]
Optimal cut-off CT number	-54	-53	-56	-67	-53
Sensitivity	15/16 (0.94) [0.90-0.97]	14/15 (0.94) [0.88-0.99]	13/14 (0.93) [0.86-0.98]	16/17 (0.94) [0.87-0.98]	51/62 (0.82) [0.76-0.90]
Specificity	43/46 (0.94) [0.89-0.98]	44/47 (0.94) [0.88-0.98]	47/48 (0.98) [0.93-1.00]	41/45 (0.91) [0.85-0.98]	176/186 (0.95) [0.89-0.99]

CT: computed tomography, AUC: area under the curve. CT numbers are given in Hounsfield units. Numbers in square brackets are confidence intervals. The quantitative image analysis showed significant differences in CT numbers with or without bone marrow edema in total and in each region ($p < .001$). The primary metrics of diagnostic accuracy such as sensitivity, specificity and the AUC were comparable in each region demonstrating excellent diagnostic accuracy of VNCA reconstructions for the depiction of traumatic calcaneal bone marrow edema in the quantitative analysis of CT numbers.

Table 4

Patient-based diagnostic accuracy results of each CT reader using color-coded VNCA reconstructions for the detection of traumatic calcaneal bone marrow edema.

	Sensitivity	Specificity	PPV	NPV	Accuracy
Average	185/195 (0.95) [0.90-0.98]	106/115 (0.92) [0.85-0.97]	185/194 (0.95) [0.91-0.98]	106/116 (0.91) [0.85-0.96]	291/310 (0.94) [0.92-0.99]
Reader 1	37/39 (0.95) [0.90-0.99]	22/23 (0.96) [0.92-0.99]	37/38 (0.97) [0.93-1.00]	22/24 (0.92) [0.85-0.98]	59/62 (0.95) [0.92-0.98]
Reader 2	38/39 (0.97) [0.93-1.00]	21/23 (0.91) [0.85-0.97]	38/40 (0.95) [0.92-0.99]	21/22 (0.96) [0.92-1.00]	59/62 (0.95) [0.90-0.99]
Reader 3	37/39 (0.95) [0.88-0.98]	21/23 (0.91) [0.84-0.96]	37/39 (0.95) [0.93-0.99]	21/23 (0.91) [0.87-0.95]	58/62 (0.94) [0.88-0.97]
Reader 4	36/39 (0.92) [0.85-0.97]	22/23 (0.96) [0.90-0.99]	36/37 (0.97) [0.94-1.00]	22/25 (0.88) [0.82-0.93]	58/62 (0.94) [0.88-0.97]
Reader 5	37/39 (0.95) [0.90-0.99]	20/23 (0.87) [0.80-0.93]	37/40 (0.93) [0.88-0.97]	20/22 (0.91) [0.86-0.95]	57/62 (0.92) [0.86-0.96]

PPV: positive predictive value, NPV: negative predictive value. Statistical measures are given as fractions and as decimal values (round brackets). Numbers in square brackets are confidence intervals.

The most experienced CT readers in this study (reader 1–3) were able to achieve excellent diagnostic performance in the detection of traumatic calcaneal bone marrow edema using VNCA reconstructions (sensitivity, specificity, PPV, NPV and accuracy, all $\geq 91\%$). Reader 1 (board-certified radiologist) had 8 years of experience in musculoskeletal (MSK) imaging; reader 2 (radiology resident), 5 years; reader 3 (radiology resident), 5 years; reader 4 (radiology resident), 3 years; reader 5 (radiology resident), 3 years.

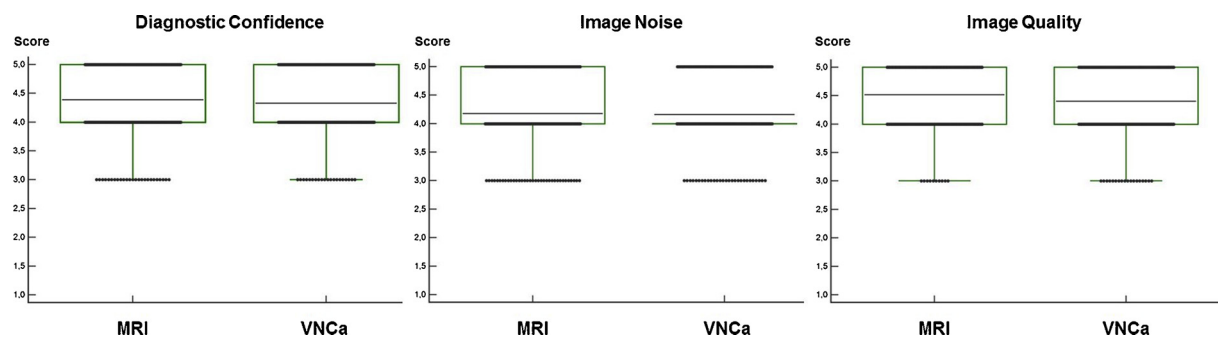


Fig. 6. Box and dot plot showing subjective image ratings concerning diagnostic confidence, amount of noise and image quality of magnetic resonance imaging (MRI) and color-coded virtual non-calcium (VNCA) reconstructions using five-point Likert scales (range 1–5; 1 = unacceptable, 5 = excellent). Color-coded VNCA reconstructions achieved comparable scores to MRI series without significant differences concerning diagnostic confidence ($p = .09$) and image noise ($p = .36$). The image quality of VNCA reconstructions was rated significantly lower compared to MRI series ($p < .001$).

imaging approach may be a viable alternative for patients with acute tarsal trauma and suspected bone marrow edema in cases in which MRI is unavailable or contraindicated but dual-energy CT can be performed.

Declaration of Competing Interest

None.

References

- [1] M. Dienst, M. Blauth, Bone bruise of the calcaneus: a case report, *Clin. Orthop. Relat. Res.* 378 (2000) 202–205, <https://doi.org/10.1097/00003086-200009000-00030>.
- [2] G. Nishimura, M. Yamato, M. Togawa, Trabecular trauma of the talus and medial malleolus concurrent with lateral collateral ligamentous injuries of the ankle: evaluation with MR imaging, *Skeletal Radiol.* 25 (1996) 49–54, <https://doi.org/10.1007/s002560050031>.
- [3] H. Pinar, D. Akseki, I. Kovanlikaya, et al., Bone bruises detected by magnetic resonance imaging following lateral ankle sprains, *Knee Surg. Sport. Traumatol. Arthrosc.* 5 (1997) 113–117, <https://doi.org/10.1007/s001670050036>.
- [4] V. Mandalia, A. Fogg, R. Chari, et al., Bone bruising of the knee, *Clin. Radiol.* 60 (2005) 627–636, <https://doi.org/10.1016/j.crad.2005.01.014>.
- [5] S.S. Boks, D. Vroegindewij, B.W. Koes, et al., Follow-up of occult bone lesions detected at MR imaging: systematic review, *Radiology* 238 (2006) 853–862, <https://doi.org/10.1148/radiol.2382050062>.
- [6] S. Eustace, C. Keogh, M. Blake, et al., MR imaging of bone oedema: mechanisms and interpretation: pictorial review, *Clin. Radiol.* 56 (2001) 4–12, <https://doi.org/10.1053/crad.2000.0585>.
- [7] R. Watura, M. Cobby, J. Taylor, Multislice CT in imaging of trauma of the spine, pelvis and complex foot injuries, *Br. J. Radiol.* 77 (2004) 46–63, <https://doi.org/10.1259/bjr/52620263>.
- [8] M.M. Leil, S.G. Ruehm, M. Kramer, et al., Cranial computed tomography angiography with automated bone subtraction: a feasibility study, *Invest. Radiol.* 44 (2009) 38–43, <https://doi.org/10.1097/rli.0b013e31818c3d6b>.
- [9] S. Nicolaou, T. Liang, D.T. Murphy, et al., Dual-energy CT: a promising new technique for assessment of the musculoskeletal system, *Am. J. Roentgenol.* 199 (2012) 78–86, <https://doi.org/10.2214/ajr.12.9117>.
- [10] P.I. Mallinson, T.M. Coupal, P.D. McLaughlin, et al., Dual-energy CT for the musculoskeletal system, *Radiology* 281 (2016) 690–707, <https://doi.org/10.1148/radiol.2016151109>.
- [11] J.L. Wichmann, C. Booz, S. Wesarg, et al., Dual-energy CT-based phantomless in vivo three-dimensional bone mineral density assessment of the lumbar spine, *Radiology* 271 (2014) 778–784, <https://doi.org/10.1148/radiol.13131952>.
- [12] C. Booz, P.C. Hofmann, M. Sedlmair, et al., Evaluation of bone mineral density of the lumbar spine using a novel phantomless dual-energy CT post-processing algorithm in comparison with dual-energy X-ray absorptiometry, *Eur. Radiol. Exp.* 1 (2017) 11, <https://doi.org/10.1186/s41747-017-0017-2>.
- [13] C. Booz, J. Nöske, S.S. Martin, et al., Virtual noncalcium dual-energy CT: detection of lumbar disk herniation in comparison with standard grayscale CT, *Radiology* 290 (2019) 446–455, <https://doi.org/10.1148/radiol.2018181286>.
- [14] J.L. Wichmann, C. Booz, S. Wesarg, et al., Quantitative dual-energy CT for phantomless evaluation of cancellous bone mineral density of the vertebral pedicle: correlation with pedicle screw pull-out strength, *Eur. Radiol.* 25 (2015) 1714–1720, <https://doi.org/10.1007/s00330-014-3529-7>.
- [15] S. Wesarg, M. Kirschner, M. Becker, et al., Dual-energy CT-based assessment of the trabecular bone in vertebrae, *Methods Inf. Med.* 51 (2012) 398, <https://doi.org/10.3414/me11-02-0034>.
- [16] B. Petritsch, A. Kosmala, A.M. Weng, et al., Vertebral compression fractures: third-generation dual-energy CT for detection of bone marrow edema at visual and quantitative analyses, *Radiology* 284 (2017) 161–168, <https://doi.org/10.1148/radiol.2017162165>.
- [17] M. Kaup, J.L. Wichmann, J.-E. Scholtz, et al., Dual-energy CT-based display of bone marrow edema in osteoporotic vertebral compression fractures: impact on diagnostic accuracy of radiologists with varying levels of experience in correlation to MR imaging, *Radiology* 280 (2016) 510–519, <https://doi.org/10.1148/radiol.2016150472>.
- [18] C.-K. Wang, J.-M. Tsai, M.-T. Chuang, et al., Bone marrow edema in vertebral compression fractures: detection with dual-energy CT, *Radiology* 269 (2013) 525–533, <https://doi.org/10.1148/radiology.13122577>.
- [19] A. Kosmala, A.M. Weng, A. Heidemeier, et al., Multiple myeloma and dual-energy CT: diagnostic accuracy of virtual noncalcium technique for detection of bone marrow infiltration of the spine and pelvis, *Radiology* 286 (2017) 205–213, <https://doi.org/10.1148/radiol.2017170281>.
- [20] C. Frellesen, M. Azadegan, S.S. Martin, et al., Dual-energy computed tomography-based display of bone marrow edema in incidental vertebral compression fractures: diagnostic accuracy and characterization in oncological patients undergoing routine staging computed tomography, *Invest. Radiol.* 53 (2018) 409–416, <https://doi.org/10.1097/rli.0000000000000458>.
- [21] R. Guggenberger, R. Gnannt, J. Hodler, et al., Diagnostic performance of dual-energy CT for the detection of traumatic bone marrow lesions in the ankle: comparison with MR imaging, *Radiology* 264 (2012) 164–173, <https://doi.org/10.1148/radiol.20110417>.

- radiol.12112217.
- [22] M.H. Albrecht, J. Trommer, J.L. Wichmann, et al., Comprehensive comparison of virtual monoenergetic and linearly blended reconstruction techniques in third-generation dual-source dual-energy computed tomography angiography of the thorax and abdomen, *Invest. Radiol.* 51 (2016) 582–590, <https://doi.org/10.1097/rli.0000000000000272>.
- [23] R. Sanders, P. Fortin, T. DiPasquale, et al., Operative treatment in 120 displaced intraarticular calcaneal fractures. Results using a prognostic computed tomography scan classification, *Clin. Orthop. Relat. Res.* 290 (1993) 87–95, <https://doi.org/10.1097/00003086-199305000-00012>.
- [24] G. Pache, B. Krauss, P. Strohm, et al., Dual-energy CT virtual noncalcium technique: detecting posttraumatic bone marrow lesions—feasibility study, *Radiology* 256 (2010) 617–624, <https://doi.org/10.1148/radiol.10091230>.
- [25] T.S. Genders, S. Spronk, T. Stijnen, et al., Methods for calculating sensitivity and specificity of clustered data: a tutorial, *Radiology* 265 (2012) 910–916, <https://doi.org/10.1148/radiol.12120509>.
- [26] J.R. Landis, G.G. Koch, The measurement of observer agreement for categorical data, *Biometrics* 33 (1977) 159–174, <https://doi.org/10.2307/2529310>.
- [27] M.H. Albrecht, C.N. De Cecco, U.J. Schoepf, et al., Dual-energy CT of the heart current and future status, *Eur. J. Radiol.* 105 (2018) 110–118, <https://doi.org/10.1016/j.ejrad.2018.05.028>.
- [28] M.S. Barr, M.W. Anderson, The knee: bone marrow abnormalities, *Radiol. Clin. North Am.* 40 (2002) 1109–1120, [https://doi.org/10.1016/s0033-8389\(02\)00051-9](https://doi.org/10.1016/s0033-8389(02)00051-9).